



## Original article

Effects of ocean acidification on the growth and biochemical composition of a green alga (*Ulva fasciata*) and its associated microbiotaKhoulood M. Barakat<sup>a</sup>, Heba S. El-Sayed<sup>a</sup>, Hanan M. Khairy<sup>a,\*</sup>, Mohamed A. El-Sheikh<sup>b</sup>, Sarah A. Al-Rashed<sup>b</sup>, Ibrahim A. Arif<sup>b</sup>, Mostafa E. Elshobary<sup>c,\*</sup><sup>a</sup> National Institute of Oceanography and Fisheries (NOIF), Cairo, Egypt<sup>b</sup> Botany & Microbiology Department, College of Science, King Saud University, Riyadh, Saudi Arabia<sup>c</sup> Botany Department, Faculty of Science, Tanta University, 31527, Tanta, Egypt

## ARTICLE INFO

## Article history:

Received 9 February 2021

Revised 11 May 2021

Accepted 12 May 2021

Available online 20 May 2021

## Keywords:

*Ulva fasciata* $p\text{CO}_2$  levels

Growth

Microbiota

Protein profile

## ABSTRACT

In marine ecosystems, fluctuations in surface-seawater carbon dioxide ( $\text{CO}_2$ ), significantly influence the whole metabolism of marine algae, especially during the early stages of macroalgal development. In this study, the response of the green alga *Ulva fasciata* for elevating ocean acidification was investigated using four levels of  $p\text{CO}_2$  ~ 280, 550, 750 and 1050  $\mu\text{atm}$ . Maximum growth rate ( $6.6\% \text{ day}^{-1}$ ), protein (32.43 % DW) and pigment (2.9 mg/g) accumulation were observed at  $p\text{CO}_2$ -550 with an increase of ~2-fold compared to control. On the other hand, lipid and carbohydrate contents recorded their maximum production (4.23 and 46.96 %DW, respectively) at  $p\text{CO}_2$ -750 while control showed 3.70 and 42.37 %DW, respectively. SDS-PAGE showed the presence of unique bands in response to  $p\text{CO}_2$ , especially at 550  $\mu\text{atm}$ . Dominant associated bacteria was shifted from *Halomonas hydrothermalis* of control to *Vibrio toranzoniae* at  $p\text{CO}_2$ -1050. These findings suggest that ocean acidification at 550  $\mu\text{atm}$  might impose noticeable effects on growth, protein, pigments, and protein profile of *U. fasciata*, which could be a good source for fish farming. While,  $p\text{CO}_2$ -750 was recommended for energetic purpose, due to its high lipid and carbohydrate contents.

© 2021 The Authors. Published by Elsevier B.V. on behalf of King Saud University. This is an open access article under the CC BY-NC-ND license (<http://creativecommons.org/licenses/by-nc-nd/4.0/>).

## 1. Introduction

Future climate forecasts expect the continuous raising of atmospheric  $\text{CO}_2$  concentrations ( $p\text{CO}_2$ ) due to the anthropogenic activities and exceed ~600 ppm by the year 2100 under the “business as usual” scenario (Pachauri et al., 2014). Oceans are one of the leading sinks of this  $\text{CO}_2$  increase as they can absorb over 25 million tons of anthropogenic  $\text{CO}_2$  daily, causing unprecedented changes to ocean chemistry (IPCC, 2007). Raised ocean  $\text{CO}_2$  concentrations modify the speciation of dissolved inorganic carbon in seawater

and reduce pH by the carbonate buffer system, along with varying abilities of macrophytes to use  $\text{CO}_2$  and  $\text{HCO}_3^-$ . By the end of the millennium, the pH of the ocean surface from a pre-industrial value (8.2) to 7.4 (Caldeira and Wickett, 2003). When pH is shifted, the carbon speciation in seawater is changed, which has strong consequences for photosynthesis, respiration, and calcification metabolism.

Additionally, these same three metabolic processes themselves change the pH of the surrounding seawater of the algae. Therefore, these changes have serious pressure on algae, including macroalgae (Kinnby et al., 2021; Xiao et al., 2021) or microalgae (Pourjamshidian et al., 2019). According to the European Water Framework Directive (EWF) 2000/60/CE, the algal community is considered an essential indicator of anthropogenic stresses in water ecosystems since it might alter the composition of their community, leading to the change or disappearance of some species (Baggini et al., 2014; Elshobary et al., 2020b; Han et al., 2020).

Seaweeds might benefit from rising  $\text{CO}_2$  through increased photosynthesis and carbon acquisition, with subsequent greater growth rates (Aires et al., 2018; Cornwall and Hurd, 2020; Mackey et al., 2015). Unlike photosynthesis, other metabolic pro-

\* Corresponding authors at: National Institute of Oceanography and Fisheries, NIOF, 11516, Egypt (H.M. Khairy), Botany Department, Faculty of Science, Tanta University, 31527, Tanta, Egypt (M.E. Elshobary).

E-mail addresses: [hanan\\_khairy@yahoo.com](mailto:hanan_khairy@yahoo.com) (H.M. Khairy), [mostafa\\_elshobary@science.tanta.edu.eg](mailto:mostafa_elshobary@science.tanta.edu.eg) (M.E. Elshobary).

Peer review under responsibility of King Saud University.



Production and hosting by Elsevier

cesses, such as ion homeostasis, respiration, nutrient uptake and enzyme activity, are suppressed by ocean acidification conditions (Fernández et al., 2015; Gutow et al., 2014; Hofmann et al., 2013). This shifting in algal metabolism may promote modifications in seaweed chemistry and change the dietary quality of tissue for grazers. In addition, association microbiota can also be influenced by environmental changes, with feedback results (Aires et al., 2018).

The Egyptian coastline of the Mediterranean (Elshobary et al., 2020a; Khairy and El-Sheikh, 2015; Osman et al., 2012), and Red Sea coasts (El-Shenody et al., 2019; Madkour et al., 2019), has a diverse variation of naturally-growing seaweed that could harvested throughout the year. *Ulva* or sea lettuce species are among the most plentiful representatives, being ubiquitous in coastal benthic communities around the world. Several *Ulva* species have been traditionally used for food and feed supplements for its high growth rate and high protein content suitable for food application (Kazir et al., 2019). Moreover, it also has several pharmaceuticals uses such as antimicrobial (Osman et al., 2013, 2012), antioxidant (Khairy and El-Sheikh, 2015), anticancer activities (Abou El Azm et al., 2019), biostimulants (Ashour et al., 2021; Hassan et al., 2021) and biofuel (Osman et al., 2020). Nonetheless, *Ulva* remains generally understudied, where *Ulva* is regarded as an attractive model organism for studying algal response and improvement against mutualistic interactions under stress conditions (Wichard et al., 2015).

This study aimed to evaluate the effects of  $p\text{CO}_2$  induced ocean acidification on *Ulva fasciata*, which is widely distributed throughout the Alexandria coast, Egypt (Osman et al., 2020, 2010, 2012). *U. fasciata* has reared under control  $p\text{CO}_2$  conditions (280  $\mu\text{atm}$ ) and three different  $p\text{CO}_2$  levels (550, 750 and 1050  $\mu\text{atm}$ ), in order to determine how *U. fasciata* may respond to  $p\text{CO}_2$  levels by evaluating algal specific growth, biochemical constituents, protein profile, and its associated microbiota which could pave the way to improve their applications.

## 2. Materials and methods

### 2.1. Algal sampling

Samples of the green macroalga *Ulva fasciata* were collected from the submerged rocks and substrates in the shallow water of the boulders at the sea anchor of the National Institute of Oceanography and Fisheries (NIOF) at 31°12'35.9"N 29°52'58.4"E, Alexandria, Egypt. The specimens have been washed immediately with seawater to eliminate sand and rock debris. The sample was preserved in a polyethylene bag filled with filtered seawater and transported to the laboratory in an icebox (5 min away). Seaweed was gently scrubbed with running filtered seawater (Whatman® GF/C glass microfiber filters, 0.5  $\mu\text{m}$ ) to clean epibiota (other seaweed, zooplankton and bivalves). All cleaned algal fronds had been blotted on towel papers to get rid of extra water and then weighed about 5 g fresh weight (FW) to start the culture experiment. The sample was adapted to lighting, temperature, and flow laboratory conditions for 48 h before evaluating its growth and biochemical composition.

### 2.2. Algal culture conditions

Adapted thalli of *U. fasciata* (equivalent to 5 g FW) was once positioned in 4 L plastic jars in triplicates and filled with filtered (Whatman® GF/C filters, 0.5  $\mu\text{m}$ ) and autoclaved seawater (salinity 30 PSU). Jars were enriched with dissolved  $p\text{CO}_2 \sim 1050, 750, 550$ , and control (280)  $\mu\text{atm}$  which organized in-stock solution then was brought in distinct concentrations to attain the desired pH val-

ues 7.2, 7.6, 7.86, 8.1 (control), respectively. Jars were covered with transparent nylon film to minimize gas exchange with the environment and subjected to the different  $p\text{CO}_2$  levels using a flowmeter gas system that mixed ambient air with 5%  $\text{CO}_2$  gas. The jars have been aerated gently via air blower to ensure a non-stop mixing of the water and preserve algal homogeneity with the experimental media. Alga used to be saved at a temperature of  $25 \pm 0.5$  °C and underneath non-stop illumination through white fluorescence lamps at 200  $\mu\text{mol photons m}^{-2} \text{s}^{-1}$ .

The experiment was performed at the National Institute of Oceanography and Fisheries (NIOF), Alexandria, Egypt, during spring 2019. Ambient pH 8.1 global levels (280  $p\text{CO}_2$ , control) and elevated  $p\text{CO}_2$  levels (550, 750 and 1050  $\mu\text{atm}$ ) related to 7.86, 7.6, 7.2, respectively were applied using acid-base addition ( $\pm 0.02$  pH units) (Smithson, 2002). Acidification levels were measured in the jars continually along the day to be always controlled in the right tested pH values. Algal total biomass in DW/L was measured during the long-term  $\text{CO}_2$  enriched seawater along 12 days culturing at three days intervals.

### 2.3. Growth measurement

The rate of *U. fasciata* growth was expressed as the specific growth rate (SGR) that was expressed as a percentage of daily increase or decrease in algal biomass (% / days intervals) as described in (Korzen et al., 2015). SGR was calculated using the following formula:

$$\text{SGR} = [\ln(W_t/W_0)]/t \times 100$$

Where  $W_t$  is the biomass (dry weight) in time per day culture and  $W_0$  is the initial biomass.  $t$  is time in days

### 2.4. Nutritional biochemical constituents

The biochemical compositions (protein, lipid, pigments and carbohydrates contents) of *U. fasciata* cultured on the different  $p\text{CO}_2$  concentrations were determined at the end of the exponential growth phase (9th day). About 5 g FW of algal sample was cut out and dried to a constant weight at 50 °C in an oven (approximately 0.5 g DW), ground to fine powder, and stored in a desiccator until further use.

#### 2.4.1. Photosynthetic pigments

Three grams of *U. fasciata* fresh weight equal to 0.3 g DW were homogenized in 30 ml acetone (80%v/v) overnight in dark at 4 °C followed by centrifugation at 10,000  $\times g$  for 5 min (TDL-8 M, Luxiangyi, Hunan, China). Chlorophyll *a* (Chl *a*), chlorophyll *b* (Chl *b*) and total carotenoids were determined spectrophotometrically (Shimadzu UV-2401PC, Kyoto, Japan) at wavelength 664, 470 and 450 nm, respectively, and expressed as mg/g DW according to (Lichtenthaler, 1987) and (Ismail and Osman, 2016).

#### 2.4.2. Total carbohydrate content

Carbohydrate content was determined by a microplate phenol-sulfuric acid method (Masuko et al., 2005) and modified by Elshobary et al. (2015). Total soluble carbohydrate was measured at 490 nm against the blank and determined per DW using glucose as a standard.

#### 2.4.3. Total lipid content

The lipid content of the macroalgal samples was measured by a solvent extraction method using Soxhlet, where petroleum ether was used as a solvent. The values are presented as a percent of the dry weight (DW) of the samples as described by (Elshobary et al., 2020a).

#### 2.4.4. Total protein content

For protein analysis, algal powder (0.5 mg DW) were digested in 1 N NaOH for 24 h at room temperature and quantified, according to Bradford methods (Bradford, 1976) modified by (Kruger, 2009). The absorbance was measured by UV/ visible spectrophotometer at 595 nm against a blank. Bovine serum albumin was used as standard, where protein content was assessed as %DW.

#### 2.5. Algal protein profile

The protein profile of the total soluble protein of *U. fasciata* under the four different acidification levels was detected via Sodium dodecyl sulfate–polyacrylamide gel electrophoresis (SDS-PAGE) (Laemmli, 1970). Ten  $\mu$ l of protein ladder (prestained dual-color standard, 14.4–116 kDa, Bio-Rad, USA) and 15  $\mu$ g of protein from each treatment were loaded onto stacking gel of 5% and separating gel of 12% acrylamide in 25 mM Tris–HCl, pH 8.3, 0.18 M Glycine and 0.1% SDS. SDS PAGE was performed using a Protean II xi cell electrophoresis unit (Biorad, Hercules, CA, USA). The separation was carried out at 180 V for 2 h. Gels were stained for 30 min with 0.02% (w/v) Coomassie Brilliant Blue R-250 in 50% (v/v) methanol and 7.5% (v/v) acetic acid, followed by a destaining for 70 min with 50% (v/v) methanol and 7.5% (v/v) acetic acid. Pictures of the gels were taken with Gel documentation system (Geldoc-it, UVP, England), which was applied for data analysis using Totallab analysis software, [www.totallab.com](http://www.totallab.com), (Ver.1.0.1).

#### 2.6. Isolation of the dominant associated bacteria

Within 2 h after collection, *Ulva* thallus was washed five times in autoclaved Petri dishes with sterilized and filtered (0.2  $\mu$ m pore size) seawater to remove loosely attached bacteria, water was exchange after each step. Rinsed samples were placed in new sterilized Petri dishes. The whole surface of the thallus was vigorously swabbed with a sterile cotton swab. Subsequently, swab tips were spread on marine agar Zobell medium (Himedia) supplemented with 1.5% agar under aseptic conditions. The plates were incubated at 20°C for three days, and the dominant colonies were purified on a fresh plate to obtain single colonies. Bacterial isolates were sustained at –20°C for molecular identification.

#### 2.7. Molecular identification of the dominant bacterial isolates

According to manufacturer protocol, DNA from bacterial isolates was obtained using GeneJET Genomic DNA Purification Kit (K0721/Thermo Fisher). PCR amplification of partial 16S rRNA gene sequences was carried out using the forward primer 27F (5'- AGAGTTTGATCCTGGCTCAG-3') and 1492R (5'- CTACGGCTACCTGTTACGA- 3'). Amplification protocol was carried out according to (Huo et al., 2020; Elshobary et al., 2015), using a thermal cycler (Applied Biosystems 2720, Foster City, CA, USA).

Agarose gel electrophoresis was used to detect the amplified products, which recovered and purified using E.Z.N.A.® Gel Extraction Kit (D2501-01). The purified DNA fragments have been sequenced directly by Macrogen Korea Company through ABI 3730XL sequencer. The sequences were blasted using the nBLAST search (<http://www.ncbi.nlm.nih.gov/blast>) to find the most homology isolates sequences available in the GenBank. The sequences have been aligned using Clustal W with the default parameters (MEGA X software) ([www.megasoftware.net](http://www.megasoftware.net)). A dendrogram was created using the neighbour-joining (NJ) algorithm based on the parameter distance (PD) using MEGA X software.

#### 2.8. Statistical analysis

All experiments were carried out in triplicates, and results were analyzed using ANOVA. To evaluate the interactive effect of age and  $p\text{CO}_2$  on SGR, two-way ANOVA was used with experimental age and  $p\text{CO}_2$  as fixed factors. Whereas, one-way ANOVA was used to assess the effect of  $p\text{CO}_2$  (fixed factor) on all biochemical components followed by Duncan and LSD (least significant difference) comparisons to determine the significance level at  $P \leq 0.05$ . The statistical analyses were done using SPSS software (version 23, SPSS Inc., USA), and data were presented as the mean  $\pm$  SD.

### 3. Results

#### 3.1. Algal growth rate

A long-term  $\text{CO}_2$  exposure test (12 days) was performed to obtain different  $p\text{CO}_2$  levels (280, 550, 750, and 1050  $\mu\text{atm}$ ) and investigate their impact on *U. fasciata* specific growth rate (SGR) (Fig. 1). In general, increasing  $\text{CO}_2$  has enhanced the growth rate than that recorded in the control treatment. The highest value (6.6%  $\text{day}^{-1}$ ) was recorded at  $p\text{CO}_2$ -550 on the 6th day with an increase of 2.7 times than control. The results also showed that the optimum SGR was obtained approximately at the 6th day of culture, where all treatments have the same exponential phase period. Otherwise, they were varied in their stationary phase durations according to their response to different  $p\text{CO}_2$  levels. The shortest stationary phase duration was noted at the highest  $p\text{CO}_2$  level (1050  $\mu\text{atm}$ ), whereas in the other treatments, it lasted till the 9th day of culture, where all the analyses in this study have been performed. The statistical analysis of two-way ANOVA indicated that the variation in  $p\text{CO}_2$  levels, age, and interaction was significantly affected SGR (ANOVA  $p < 0.001$ ) (Table S1).

#### 3.2. Biochemical constituents and pigment contents of *U. Fasciata*

The photosynthetic pigments of *U. fasciata* were significantly affected by  $p\text{CO}_2$  levels (ANOVA  $p < 0.05$ ). The pigment content of *U. fasciata* thalli was increased dramatically than ambient condition. The maximum Chl *a*, Chl *b*, carotenoids and total pigments (1.95, 0.93, 0.054, 2.9 mg/g respectively) were recorded at  $p\text{CO}_2$ -550 (Fig. 2), with an increase of 107%, 55% and 1%, respectively than recorded in control. While rising  $p\text{CO}_2$  over 550 causes a reduction in pigment content. In general, raising  $p\text{CO}_2$  enhanced 550  $\mu\text{atm}$  attained the maximum pigment production.

Total protein, lipid and carbohydrate contents of the *U. fasciata* were significantly improved by applying different  $p\text{CO}_2$  levels (ANOVA  $p < 0.05$ ). Higher protein accumulation was found at  $p\text{CO}_2$ -550  $\mu\text{atm}$  (32.43%DW) with an increase of 1.2-fold than recorded in control. In contrast, the protein content was decreased by increasing  $p\text{CO}_2$  levels over 550  $\mu\text{atm}$  (Table 1). On the other hand, the lipid and carbohydrate contents of *U. fasciata* were improved significantly by elevated  $p\text{CO}_2$ . Their highest values (4.23 and 46.96 %DW, respectively) were recorded at  $p\text{CO}_2$ -750 (Table 1). Even though the most elevated  $\text{PCO}_2$  of 1050  $\mu\text{atm}$  recorded lipid and carbohydrate yield below 750  $\mu\text{atm}$ , they were still higher than those observed in the control treatment. Table 2.

#### 3.3. Protein profile analysis

Protein profile analysis was determined using SDS-PAGE. In general, the most abundant protein bands had weights of 35, 32.5, 31, 22.4 kDa. Comparing to control, different unfamiliar and unique protein bands were expressed and reflected by different  $p\text{CO}_2$  values of *U. fasciata* culturing media (Fig. 3). Treating with

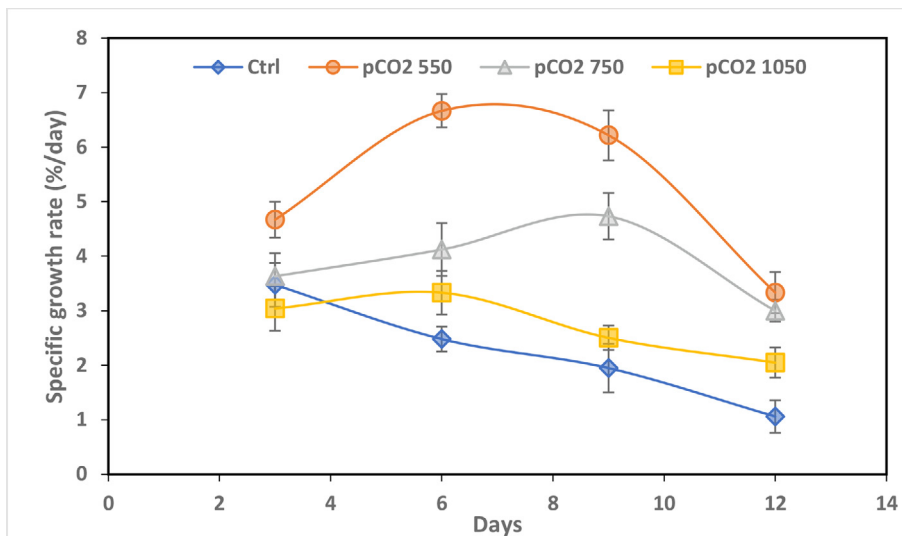


Fig. 1. Specific growth rate of *U. fasciata* (%/ day) cultured for 12 days on different pCO<sub>2</sub> levels.

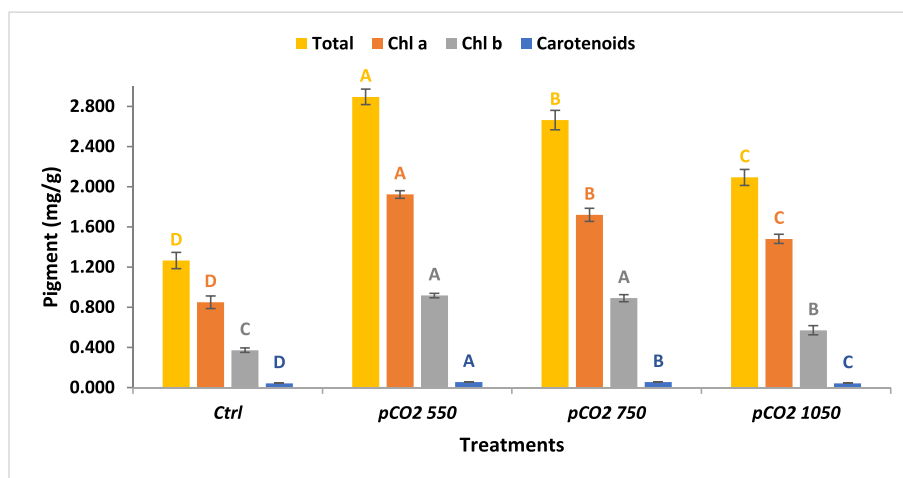


Fig. 2. Pigment content of *U. fasciata* under different pCO<sub>2</sub> concentrations.

Table 1  
Biochemical constituents of *U. fasciata* cultured on different pCO<sub>2</sub> concentrations.

Treatment pCO <sub>2</sub>	Protein (%DW)	Lipid (%DW)	Carbohydrate (%DW)
Control (pCO <sub>2</sub> 280)	26.99 ± 0.23 <sup>c</sup>	3.70 ± 0.04 <sup>c</sup>	42.34 ± 0.21 <sup>c</sup>
pCO <sub>2</sub> 550	32.43 ± 0.27 <sup>a</sup>	3.90 ± 0.03 <sup>b</sup>	46.04 ± 0.17 <sup>b</sup>
pCO <sub>2</sub> 750	28.70 ± 0.48 <sup>b</sup>	4.23 ± 0.05 <sup>a</sup>	46.96 ± 0.09 <sup>a</sup>
pCO <sub>2</sub> 1050	21.53 ± 0.20 <sup>d</sup>	3.93 ± 0.04 <sup>b</sup>	46.13 ± 0.11 <sup>b</sup>
F- value	610.00*	126.68*	559.68*
LSD	0.26	0.28	0.12

pCO<sub>2</sub> 550 μatm reflected the highest number of bands (13 bands) with unique five bands at 59, 42, 26.5, 26 and 20 KDa. Interestingly, all pCO<sub>2</sub> treatments showed a unique band at 20 KDa that was not

observed in control. However, the other treatment and control reflected only 11 bands but at different molecular weights. Only one unique fraction with 27 KDa was distinguished in medium with pCO<sub>2</sub>-750. Two unique fractions with 48 and 28 KDa were reflected by pCO<sub>2</sub>-1050 (Fig. 3).

### 3.4. Bacterial identification

As shown in Table (2), bacterial consortium associated with *U. fasciata* in control and different pCO<sub>2</sub> concentrations were identified by amplifying the 16S rDNA gene and aligned with the close related strains (Fig. 4). The dominant bacterium was identified in each treatment. The 16S rRNA gene phylogeny was inferred from

Table 2  
Sequence identity of the dominate associated bacteria within *U. fasciata* thallus using a comparison with most identity GenBank accessions.

Treatments	Identified strain with the highest identity	Max Score	Total Score	Query Cover	E value	Identity %	Accession number
Control (pCO <sub>2</sub> 280)	<i>Halomonas hydrothermalis</i>	1105	6610	100%	0.0	100.00%	AP022843
pCO <sub>2</sub> -550	<i>Halomonas venusta</i>	761	761	100%	0.0	99.76%	MT510186
pCO <sub>2</sub> -750	<i>Halomonas venusta</i>	981	981	100%	0.0	100.00%	MT299647
pCO <sub>2</sub> -1050	<i>Vibrio campbellii</i>	761	761	100%	0.0	99.76%	MT510186

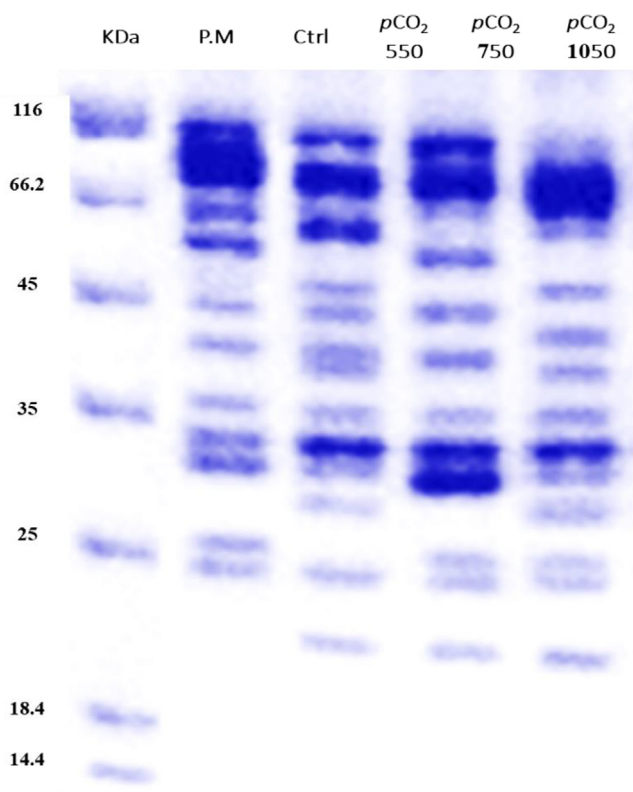


Fig. 3. Protein fingerprinting patterns for *U. fasciata* under different  $p\text{CO}_2$ . PM, protein marker.

about 500 bp nucleotide sequences (PCR-based) that originated from four predominant bacterial isolates. From the maximum neighbor joint phylogenetic tree based on the 16S rRNA gene, the 16S gene region was aligned with 16S nucleotide sequences of 29 bacterial strains in the NCBI Ribosomal RNA sequence. The phylogenetic tree consisted of two main clades the first clade of *Halomonas* sp., where the dominant strain of moderate  $p\text{CO}_2$  level (550 and 750  $\mu\text{atm}$ ) was grouped with *Halomonas venusta* (MK357745, MF928305, MF928305 and LN995436) with identity percentages reached up to 99%, respectively and bootstrap of 77. While, the dominant strain of control was grouped with *Halomonas hydrothermalis* (AP022843) with 100% similarity percentage and 91 bootstraps. The second clade was grouped the dominate species of the highest  $p\text{CO}_2$  level (1050  $\mu\text{atm}$ ) with *Vibrio toranzoniae* (MT510186, LR722816 and MN945290) that showed identity percentage reached to 99% and bootstrap of 92%. From the above results,  $p\text{CO}_2$  variation has a significant effect on *U. fasciata* associated bacteria consortium.

#### 4. Discussion

In marine ecosystems, enrichment of different  $\text{CO}_2$  in seawater levels consequently affects the acidification of seawater, which influences marine algae metabolism. The overgrowth of *Ulva* sp. in response to elevated  $p\text{CO}_2$  in eutrophic estuaries can be directly promoted by acidification (Young and Gobler, 2016a). However, Reidenbach et al. (2017) detected no changes in *U. australis* growth by decreasing  $p\text{CO}_2$ , which influenced the carbon and nitrogen metabolisms. Also, Chen et al. found that both lowered and increased seawater pH exert significant physiological stress on *U. lactuca* germlings (Chen et al., 2017).

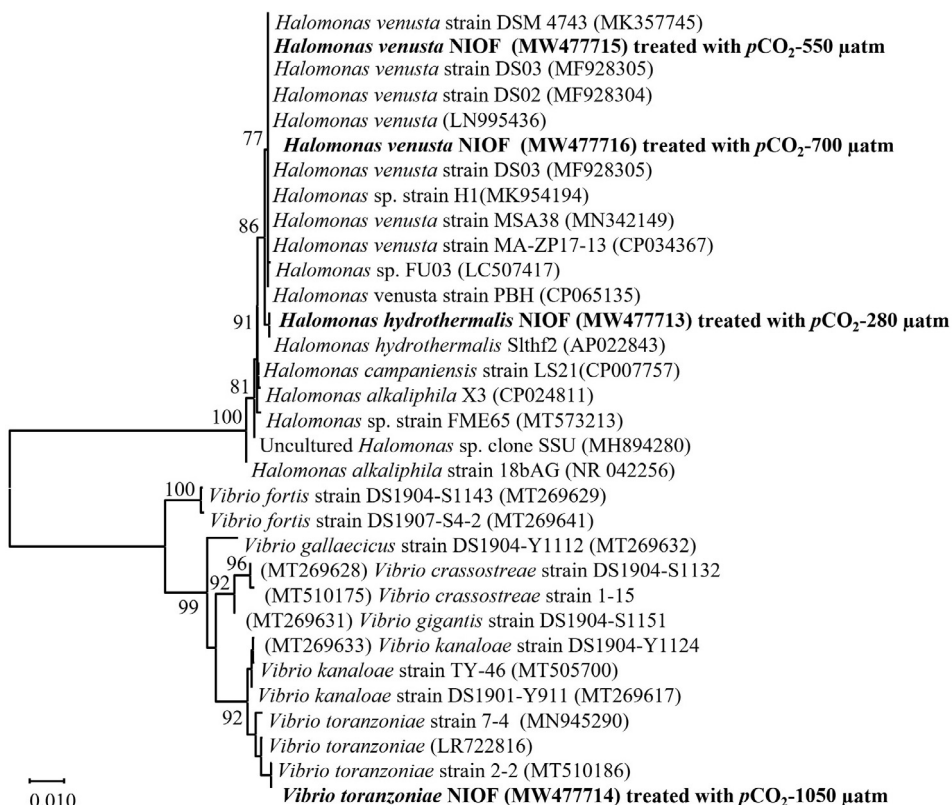


Fig. 4. Neighbour-joining (NJ) dendrogram was constructed for the dominant bacterial strains based on 16S rRNA nucleotide sequences. Bootstrap values higher than 70 are shown on the trees.

In this study, CO<sub>2</sub> enrichment enhanced the growth rate of *Ulva fasciata* than recorded in the control and the highest value (6.6% day<sup>-1</sup>) was recorded at pCO<sub>2</sub>-550 on the 6th day with an increase of more than double folds than control. In this regard, Young and Gobler (2016) reported that *Gracilaria* and *Ulva*'s growth rates were significantly boosted by an average of 70% and 30%, respectively, beyond control treatment when exposed to raised levels of pCO<sub>2</sub>. Furthermore, *Gracilaria* and *Ulva* show a physiological shift from near-exclusive use of HCO<sub>3</sub><sup>-</sup> to mainly CO<sub>2</sub> use when subjected to elevated pCO<sub>2</sub> via detecting δ<sup>13</sup>C isotopes. This shift in carbon dependence coupled with growth rate increased in response to increased pCO<sub>2</sub>, proposed that these seaweeds' photosynthesis depended on their inorganic carbon source (Young and Gobler, 2016a). Semesi et al. (2009) demonstrated that increasing dissolved CO<sub>2</sub> concentration to a specific level of ~ 26 μmol kg<sup>-1</sup> caused enhancing the photosynthetic rates of *Hydrolythion* sp by 13%. Additionally, the negative impact of the higher pCO<sub>2</sub> on the growth of *U. fasciata* in the present study may contribute to the lowered pH. Elevated pCO<sub>2</sub> reduces pH at the surface of the cell, which could modify both extracellular and intracellular acid-base balance (Flynn et al., 2012). Intracellular metabolic activities, including photosynthesis and development, may be impaired by disrupted homeostasis (Z. Xu et al., 2017). A reduced growth rate caused by decreased pH was also found in different seaweed such as *Pyropia yezoensis* (G. Gao et al., 2019), *P. haitanensis* (K. Xu et al., 2017) and *U. lactuca* (Olischläger et al., 2013).

The marine macroalga *Ulva* sp. is a candidate raw biomass with a high growth rate and high protein, lipid, carbohydrate yield suitable for food application (Kazir et al., 2019; Khairy and El-Shafay, 2013). A recent study showed that pH-shift of *Ulva* sp improves the nutrient contents and gives a high grade of food applications (Harrysson et al., 2019).

Color and flavor are essential criteria in determining seaweed feed and food qualities and thus, market value. Seaweeds with a darker color and more protein are favorable by consumers and have a higher value in the market. The color of seaweeds is mainly determined by photosynthetic pigments, such as chlorophyll and carotenoids (Niwa and Harada, 2013). Regarding algal pigments, chlorophyll *a*, *b* and carotenoids contents of *U. fasciata* thalli were significantly differentiated at a different level of pCO<sub>2</sub>, the maximum Chl *a*, Chl *b* and carotenoids were recorded at pCO<sub>2</sub>-550 and declined by elevating the pCO<sub>2</sub> level. This finding was in accordance (G. Gao et al., 2019; K. Gao et al., 2019) who recorded that increasing pCO<sub>2</sub> concentration improved the color and flavor of edible red algae *Pyropia yezoensis* by boosting pigments, and amino acids contents. In brown seaweed *Sargassum vulgare*, photosynthetic pigments have improved at the acidified site than alkaline one (Kumar et al., 2020). On contrary, raising pCO<sub>2</sub> to 750 μatm, the pigment content was decreased. The same finding was recorded in *U. lactuca*, where both Chl *a* and Chl *b* content were reduced at 750 μatm at the end of the experiment (Olischläger et al., 2013).

Carbohydrate is the main calorific compound in seaweeds that are utilized in metabolism as a source of energy needed for respiration and other important processes (Sudhakar et al., 2019) as well as soluble carbohydrates can serve as precursors for bioactive metabolites (Kumar et al., 2020). Seaweeds carbohydrate is a valuable and sustainable source for pharmaceutical, cosmeceutical, and traditional applications (Ahmed et al., 2014) and bioethanol feedstock (Elshobary et al., 2020a; Osman et al., 2020). The results showed that the carbohydrate was the most dominant component in *U. fasciata*. This finding is agreed with results of (Osman et al., 2020) who observed that the carbohydrate content of *U. fasciata* ranged from 37.1%DW during winter to 40.46 %DW during summer, while *U. rigida* sp. showed lower trends of carbohydrates 28.6% when cultivated under fish effluents compared to the control

site (Korzen et al., 2015). Different levels of pCO<sub>2</sub> showed a significant effect on the carbohydrate content and the highest carbohydrate content (46.96%DW) was demonstrated at 750 μatm. In a recent study, the content of fucoidan and alginate polysaccharides were higher in the algal community of acidified environment (Kumar et al., 2020). Rogers et al. (1998) and Webber et al. (1994) found that elevating CO<sub>2</sub> can decrease RuBisCO concentrations; however, it can lead to an increase in soluble carbohydrate content, which can increase the total carbon content of algal tissue. In contrast, pCO<sub>2</sub> did not affect carbohydrate content in *U. rigida* (Gao et al., 2017). These differences may be depending on acclimation ability of each species to the different degrees of pCO<sub>2</sub>. Although there is no clear metabolic understanding of the relationship between CO<sub>2</sub> concentrations and cell wall carbohydrates, it has been documented that elevated CO<sub>2</sub> concentrations may enhance the activity of enzymes responsible for the synthesis of cell wall uronic acid, resulting in increased cell wall carbohydrate synthesis (Cheng et al., 2015). Another research discovered that under elevated acidification level, genes encoding enzymes involved in cell wall formation and structure, as well as carbon storage, were expressed at higher levels in *Sargassum vulgare* than under control conditions (Kumar et al., 2017).

In macroalgae, the lipids constitute a suitable storage material widely distributed, in different macroalgal classes (Sudhakar et al., 2019). Lipid is a calorific component that can be used for aquaculture (El-Khodary et al., 2020) or feedstock for biodiesel (Essa et al., 2018; Ashour et al., 2019; Elshobary et al., 2019; Huo et al., 2020). Despite the current study observed low lipid content (4.23 %DW), this is comparable with other reports, which showed the lipid content of macroalgae were <5% of dry weight (Elshobary et al., 2020a; Khairy and El-Shafay, 2013; Osman et al., 2020). The differences in lipid reported quantities could be due to several factors such as seasonal and geographical factors, climate change, and the development stage of the macroalgae (Osman et al., 2020). Noteworthy, the increase in ocean acidity combined with an increase in the lipid content, showing the maximum value at pCO<sub>2</sub>-750 with a rise of 54% than that were found in control. Gao et al. (2017) observed that increasing pCO<sub>2</sub> up to pH 7.95 increased lipid content in *U. rigida* under the high temperature by 22.55% than low pCO<sub>2</sub> treatments. Gordillo et al. (2001a) detected that under different pCO<sub>2</sub> levels, significant changes were observed in total lipid content as well as its classes in *U. rigida*. Triglycerides accumulated at high CO<sub>2</sub> and under nitrogen deficient, while chloroplast-related lipids recorded an inverse response. In general, high pCO<sub>2</sub> concentration of 1000 ppm showed a negative impact on total lipid accumulation.

Protein plays crucial roles in all algal biological processes; their activities can be described by transport and storage, enzymatic catalysis, and mechanical sustentative control (Sudhakar et al., 2019). The current study revealed that *U. fasciata* accumulated the highest protein content of 32.43%DW, at pCO<sub>2</sub>-550 compared with high pCO<sub>2</sub> levels and control synchronized with the growth rate. A recent study showed that ocean acidification of *Ulva* sp. improves the protein yield to 29% by 2.3-fold higher than recorded by control and gives a high grade of food applications (Harrysson et al., 2019). Gao et al., (2017) reported that protein levels were increased in *U. rigida* in response to pH-shifting. In contrast, high CO<sub>2</sub> upto 10,000 ppm reduced total soluble protein compared to the ambient CO<sub>2</sub> level of 350 ppm (Gordillo et al., 2001b, 2001a). The reduction in protein content under high CO<sub>2</sub> level may be attributed to the algal species tends to accumulate some biochemical such carbohydrate and lipid over the others (protein) under high CO<sub>2</sub> concentration. In this regard, Chen et al. observed that, carbohydrate content increased in *Pyropia haitanensis* while protein content decreased due to higher dissolved inorganic carbon in highly acidified seawater (Chen et al., 2019b). Several studies

observed the same results (Chen et al., 2019a; Duarte et al., 2016; Gao et al., 2018b, 2018a). This may be explained by increasing CO<sub>2</sub> concentration increases the CO<sub>2</sub> passive diffusion, resulting in a reduction in active transport proteins inside the seaweed's cell and allocating more energy for growth (Young and Gobler, 2016b). These results are also consistent with the SDS-PAGE which showed the largest number of unique protein bands were detected in the moderate pCO<sub>2</sub> level (550 μatm) and these bands reduced by increasing pCO<sub>2</sub> level.

The ability of seaweed to different biochemical stresses may be due to symbiosis with microbiota (Dominguez and Loret, 2019). Interactions between *Ulva* spp. and their associated bacteria have been well-characterized over the last decade, where bacterial colonization has been defined based on 16S rRNA gene phylogeny (Wichard et al., 2015). The interconnected evolutionary history of algae and bacteria allowed a wide range of associations to be established, characterized by the coordinated exchange of nutrients and mutual support for growth factors (Cirri and Pohnert, 2019; Huo et al., 2020). Many studies stated that different compositions of bacterial communities could enable *Ulva* species to support the 'competitive lottery' theory for how symbiotic bacteria help algae in either ambient or harsh conditions (Comba-González et al., 2016; Ghaderiardakani et al., 2017; Kessler et al., 2018; Spoerner et al., 2012). As a result of acidification, the seaweed-associated bacterial community had changed, where, elevating CO<sub>2</sub> altered the dominant associated bacteria from *Halomonas* sp. of ambient condition (280 μatm) and moderate pCO<sub>2</sub> (550–750 μatm) to *Vibrio toranzoniae* at the highest pCO<sub>2</sub> level (1050 μatm). This finding is in accordance with (Aires et al., 2018) who observed that the bacterial community of *Sargassum muticum* was changed, where Oceanospirillales and Vibrionales significantly increased their abundance in acidified conditions. Vibrionales, usually associated with diseased seaweeds, proposing that acidification may facilitate opportunistic/pathogenic bacteria. Moreover, Alpha diversity of total bacteria communities and Cyanobacteria communities was significantly varied among different pH/CO<sub>2</sub> sites (Taylor et al., 2014). Coral microbiomes contribute to seaweed adaptation to environmental change, especially pH/CO<sub>2</sub> levels (Biagi et al., 2020).

## 5. Conclusion

From the above results, it could be concluded that a considerable influence of pCO<sub>2</sub> on the whole performance of *U. fasciata*, including growth rate, protein, pigment, lipid and carbohydrate, and associated microbiota. Ocean acidification at pCO<sub>2</sub>-550 μatm is the optimum concentration to improving growth, protein and pigment contents and protein profile which could be a good source for alimentary fish source. While elevating ocean acidification to pCO<sub>2</sub>-750 μatm could be preferable for bioenergy production by stimulating energetic compounds of lipid and carbohydrate.

## Declaration of Competing Interest

The authors declare that they have no known competing financial interests or personal relationships that could have appeared to influence the work reported in this paper.

## Acknowledgements

Authors kindly acknowledge the support of the Saudi Biological Society, King Saud University, Riyadh, Saudi Arabia of this research.

## Appendix A. Supplementary data

Supplementary data to this article can be found online at <https://doi.org/10.1016/j.sjbs.2021.05.029>.

## References

- Abou El Azm, N., Fleita, D., Rifaat, D., Mpingirika, E.Z., Amleh, A., El-Sayed, M.M.H., 2019. Production of bioactive compounds from the sulfated polysaccharides extracts of *Ulva lactuca*: Post-extraction enzymatic hydrolysis followed by ion-exchange chromatographic fractionation. *Molecules* 24, 2132.
- Aires, T., Serebryakova, A., Viard, F., Serrão, E.A., Engelen, A.H., 2018. Acidification increases abundances of Vibrionales and Planctomycetia associated to a seaweed-grazer system: potential consequences for disease and prey digestion efficiency. *PeerJ* 6. <https://doi.org/10.7717/peerj.4377>.
- Ashour, M., Elshobary, M.E., El-Shenody, R., Kamil, A.W.A., Abomohra, A.E., 2019. Evaluation of a native oleaginous marine microalga *Nannochloropsis oceanica* for dual use in biodiesel production and aquaculture feed. *Biomass and Bioenergy* 120, 439–447. <https://doi.org/10.1016/j.biombioe.2018.12.009>.
- Ashour, Mohamed, Hassan, Shima M., Elshobary, Mostafa E., Ammar, Gamal A.G., Gaber, Ahmed, Alsanie, Walaa F., Mansour, Abdallah Tageldein, El-Shenody, Rania, 2021. Impact of commercial seaweed liquid extract (TAM®) biostimulant and its bioactive molecules on Growth and Antioxidant Activities of Hot Pepper (*Capsicum annum*). *Plants* 10 (1045). <https://doi.org/10.3390/plants10061045>.
- Baggini, C., Salomidi, M., Voutsinas, E., Bray, L., Kraskopoulou, E., Hall-Spencer, J.M., 2014. Seasonality affects macroalgal community response to increases in pCO<sub>2</sub>. *PLoS One* 9, 1–13. <https://doi.org/10.1371/journal.pone.0106520>.
- Biagi, E., Caroselli, E., Barone, M., Pezzimenti, M., Teixido, N., Soverini, M., Rampelli, S., Turroni, S., Gambi, M.C., Brigidi, P., Goffredo, S., Candela, M., 2020. Patterns in microbiome composition differ with ocean acidification in anatomic compartments of the Mediterranean coral *Astroires calycularis* living at CO<sub>2</sub> vents. *Sci. Total Environ.* 724. <https://doi.org/10.1016/j.scitotenv.2020.138048>.
- Bradford, M.M., 1976. A rapid and sensitive method for the quantitation of microgram quantities of protein utilizing the principle of protein-dye binding. *Anal. Biochem.* 72, 248–254.
- Caldeira, K., Wickett, M.E., 2003. Anthropogenic carbon and ocean pH. *Nature* 425, 365.
- Chen, B., Lin, L., Ma, Z., Zhang, T., Chen, W., Zou, D., 2019a. Carbon and nitrogen accumulation and interspecific competition in two algae species, *Pyropia haitanensis* and *Ulva lactuca*, under ocean acidification conditions. *Aquac. Int.* 27, 721–733. <https://doi.org/10.1007/s10499-019-00360-y>.
- Chen, B., Xia, J., Zou, D., Zhang, X., 2019b. Responses to ocean acidification and diurnal temperature variation in a commercially farmed seaweed, *Pyropia haitanensis* (Rhodophyta). *Eur. J. Phycol.* 54, 184–192. <https://doi.org/10.1080/09670262.2018.1539250>.
- Chen, B., Zou, D., Zhu, M., 2017. Growth and photosynthetic responses of *Ulva lactuca* (Ulinales, Chlorophyta) germlings to different pH levels. *Mar. Biol. Res.* 13, 351–357. <https://doi.org/10.1080/17451000.2016.1267367>.
- Cheng, Y.-S., Labavitch, J.M., VanderCheynst, J.S., 2015. Elevated CO<sub>2</sub> concentration impacts cell wall polysaccharide composition of green microalgae of the genus *Chlorella*. *Lett. Appl. Microbiol.* 60, 1–7. <https://doi.org/10.1111/lam.12320>.
- Cirri, E., Pohnert, G., 2019. Algae–bacteria interactions that balance the planktonic microbiome. *New Phytol.* 223, 100–106. <https://doi.org/10.1111/nph.15765>.
- Comba-González, N.B., Ruiz-Toquica, J.S., Lopez-Kleine, L., Montoya-Castano, D., 2016. Epiphytic bacteria of macroalgae of the genus *Ulva* and their potential in producing enzymes having biotechnological interest. *J. Mar. Biol.*, 2–9.
- Cornwall, C.E., Hurd, C.L., 2020. Variability in the benefits of ocean acidification to photosynthetic rates of macroalgae without CO<sub>2</sub>-concentrating mechanisms. *Mar. Freshw. Res.* 71, 275–280. <https://doi.org/10.1071/MF19134>.
- Dominguez, H., Loret, E.P., 2019. *Ulva lactuca*, A Source of Troubles and Potential Riches. *Mar. Drugs* 17, 1–20. <https://doi.org/10.3390/md17060357>.
- Duarte, C., López, J., Benítez, S., Manríquez, P.H., Navarro, J.M., Bonta, C.C., Torres, R., Quijón, P., 2016. Ocean acidification induces changes in algal palatability and herbivore feeding behavior and performance. *Oecologia* 180, 453–462. <https://doi.org/10.1007/s00442-015-3459-3>.
- El-Khodary, G.M., El-Sayed, H.S., Khairy, H.M., El-Sheikh, M.A., Qi, X., Elshobary, M.E., 2020. Comparative study on growth, survival and pigmentation of *Solea aegyptiaca* larvae by using four different microalgal species with emphasize on water quality and nutritional value. *Aquac. Nutr. anu.13211*. <https://doi.org/10.1111/anu.13211>.
- El-Shenody, RA, Ashour, M, Ghobara, MME, 2019. Evaluating the chemical composition and antioxidant activity of three Egyptian seaweeds: *Dictyota dichotoma*, *Turbinaria decurrens*, and *Laurencia obtusa*. *Brazilian Journal of Food Technology* 22. <https://doi.org/10.1590/1981-6723.20318>.
- Elshobary, M.E., Abo-Shady, A.M., Khairy, H.M., Essa, D., Zabed, H.M., Qi, X., Abomohra, A.E., 2019. Influence of nutrient supplementation and starvation conditions on the biomass and lipid productivities of *Micractinium reisseri* grown in wastewater for biodiesel production. *J. Environ. Manage.* 250. <https://doi.org/10.1016/j.jenvman.2019.109529>.
- Elshobary, M.E., El-Shenody, R., Abomohra, A.E., 2020a. Sequential biofuel production from seaweeds enhances the energy recovery : A case study for biodiesel and bioethanol production. *Int. J. Energy Res.* 1–11. <https://doi.org/10.1002/er.6181>.

- Elshobary, M.E., Essa, D.I., Attiah, A.M., Salem, Z.E., Qi, X., 2020b. Algal community and pollution indicators for the assessment of water quality of Ismailia canal. *Egypt. Stoch. Environ. Res. Risk Assess.* 34, 1089–1103. <https://doi.org/10.1007/s00477-020-01809-w>.
- Elshobary, M.E., Osman, M.E.H., Abushady, A.M., Piercey-Normore, M.D., 2015. Comparison of lichen-forming cyanobacterial and green algal photobionts with free-living algae. *Cryptogam. Algal.* 36, 81–100. <https://doi.org/10.7872/crya.v36.iss1.2015.81>.
- Essa, Dorya, Abo-Shady, Atef, Khairy, Hanan, Abomohra, Abd El-Fatah, Elshobary, Mostafa, 2018. Potential cultivation of halophilic oleaginous microalgae on industrial wastewater. *Egyptian Journal of Botany* 58 (2), 205–216. <https://doi.org/10.21608/ejbo.2018.809.1054>.
- Fernández, P.A., Roleda, M.Y., Hurd, C.L., 2015. Effects of ocean acidification on the photosynthetic performance, carbonic anhydrase activity and growth of the giant kelp *Macrocystis pyrifera*. *Photosynth. Res.* 124, 293–304. <https://doi.org/10.1007/s11120-015-0138-5>.
- Flynn, K.J., Blackford, J.C., Baird, M.E., Raven, J.A., Clark, D.R., Beardall, J., Brownlee, C., Fabian, H., Wheeler, G.L., 2012. Changes in pH at the exterior surface of plankton with ocean acidification. *Nat. Clim. Chang.* 2, 510–513.
- Gao, G., Clare, A.S., Chatzidimitriou, E., Rose, C., Caldwell, G., 2018a. Effects of ocean warming and acidification, combined with nutrient enrichment, on chemical composition and functional properties of *Ulva rigida*. *Food Chem.* 258, 71–78. <https://doi.org/10.1016/j.foodchem.2018.03.040>.
- Gao, G., Clare, A.S., Rose, C., Caldwell, G.S., 2018b. *Ulva rigida* in the future ocean: potential for carbon capture, bioremediation and biomethane production. *GCB Bioenergy* 10, 39–51. <https://doi.org/10.1111/gcbb.12465>.
- Gao, G., Clare, A.S., Rose, C., Caldwell, G.S., 2017. Eutrophication and warming-driven green tides (*Ulva rigida*) are predicted to increase under future climate change scenarios. *Mar. Pollut. Bull.* 114, 439–447. <https://doi.org/10.1016/j.marpolbul.2016.10.003>.
- Gao, G., Gao, Q., Bao, M., Xu, J., Li, X., 2019a. Nitrogen availability modulates the effects of ocean acidification on biomass yield and food quality of a marine crop *Pyropia yezoensis*. *Food Chem.* 271, 623–629. <https://doi.org/10.1016/j.foodchem.2018.07.090>.
- Gao, K., Beardall, J., Häder, D.-P., Hall-Spencer, J.M., Gao, G., Hutchins, D.A., 2019b. Effects of ocean acidification on marine photosynthetic organisms under the concurrent influences of warming, UV radiation, and deoxygenation. *Front. Mar. Sci.* 6, 322.
- Ghaderiardakani, F., Coates, J.C., Wichard, T., 2017. Bacteria-induced morphogenesis of *Ulva intestinalis* and *Ulva mutabilis* (Chlorophyta): a contribution to the lottery theory. *FEMS Microbiol. Ecol.* 93.
- Gordillo, F.J.L., Jiménez, C., Goutx, M., Niell, X., 2001a. Effects of CO<sub>2</sub> and nitrogen supply on the biochemical composition of *Ulva rigida* with especial emphasis on lipid class analysis. *J. Plant Physiol.* 158, 367–373.
- Gordillo, F.J.L., Niell, F.X., Figueroa, F.L., 2001b. Non-photosynthetic enhancement of growth by high CO<sub>2</sub> level in the nitrophilic seaweed *Ulva rigida* C. Agardh (Chlorophyta). *Planta* 213, 64–70.
- Gutw, L., Rahman, M.M., Bartl, K., Saborowski, R., Bartsch, I., Wiencke, C., 2014. Ocean acidification affects growth but not nutritional quality of the seaweed *Fucus vesiculosus* (Phaeophyceae, Fucales). *J. Exp. Mar. Biol. Ecol.* 453, 84–90. <https://doi.org/10.1016/j.jembe.2014.01.005>.
- Han, T., Shi, R., Qi, Z., Huang, H., Wu, F., Gong, X., 2020. Biogenic acidification of Portuguese oyster *Magallana angulata* mariculture can be mediated through introducing brown seaweed *Sargassum hemiphyllum*. *Aquaculture* 520, 734972.
- Harrysson, H., Konasani, V.R., Toth, G.B., Pavia, H., Albers, E., Undeland, I., 2019. Strategies for Improving the Protein Yield in pH-Shift Processing of *Ulva lactuca* Linnaeus: Effects of Ulvan Lyases, pH-Exposure Time, and Temperature. *ACS Sustain. Chem. Eng.* 7, 12688–12691.
- Hassan, Shima M, Ashour, Mohamed, Soliman, Ahmed A F, Hassanien, Hesham A, Alsanie, Walaa F, Gaber, Ahmed, Elshobary, Mostafa E, 2021. The potential of a new commercial seaweed extract in stimulating morpho-agronomic and bioactive properties of *Erica vesicularis* (L.) Cav. *Sustainability* 13, (8). <https://doi.org/10.3390/su13084485>.
- Hofmann, L.C., Straub, S., Bischof, K., 2013. Elevated CO<sub>2</sub> levels affect the activity of nitrate reductase and carbonic anhydrase in the calcifying rhodophyte *Corallina officinalis*. *J. Exp. Bot.* 64, 899–908. <https://doi.org/10.1093/jxb/ers369>.
- Huo, S., Basheer, S., Liu, F., Elshobary, M., Zhang, C., Qian, J., Xu, L., Arslan, M., Cui, F., Zan, X., Zhu, F., Zou, B., Ding, Q., Ma, H., 2020. Bacterial intervention on the growth, nutrient removal and lipid production of filamentous oleaginous microalgae *Tribonema* sp. *Algal Res.* 52. <https://doi.org/10.1016/j.algal.2020.102088>.
- IPCC, 2007. (Intergovernmental Panel on Climate Change) Climate Change 2007 Synthesis Report [WWW Document]. Cambridge Univ. Press. New York.
- Ismail, M.M., Osman, M.E.H., 2016. Seasonal fluctuation of photosynthetic pigments of most common red seaweeds species collected from Abu Qir, Alexandria. *Egypt. Rev. Biol. Mar. Oceanogr.* 51, 515–525. <https://doi.org/10.4067/S0718-19572016000300004>.
- Kazir, M., Abuhassira, Y., Robin, A., Nahor, O., Luo, J., Israel, A., Golberg, A., Livney, Y. D., 2019. Extraction of proteins from two marine macroalgae, *Ulva* sp. and *Gracilaria* sp., for food application, and evaluating digestibility, amino acid composition and antioxidant properties of the protein concentrates. *Food Hydrocoll.* 87, 194–203.
- Kessler, R.W., Weiss, A., Kuegler, S., Hermes, C., Wichard, T., 2018. Macroalgal-bacterial interactions: role of dimethylsulfoniopropionate in microbial gardening by *Ulva* (Chlorophyta). *Mol. Ecol.* 27, 1808–1819.
- Khairy, H.M., El-Shafay, S.M., 2013. Seasonal variations in the biochemical composition of some common seaweed species from the coast of Abu Qir Bay, Alexandria. *Oceanologia* 55, 435–452.
- Khairy, H.M., El-Sheikh, M.A., 2015. Antioxidant activity and mineral composition of three Mediterranean common seaweeds from Abu-Qir Bay, Egypt. *Saudi J. Biol. Sci.* 22, 623–630. <https://doi.org/10.1016/j.sjbs.2015.01.010>.
- Khairy, H.M., El-Sheikh, M.A., 2015. Antioxidant activity and mineral composition of three Mediterranean common seaweeds from Abu-Qir Bay, Egypt. *Saudi Journal of Biological Sciences* 22 (2), 623–630. <https://doi.org/10.1016/j.sjbs.2015.01.010>.
- Kinby, A., White, J.C.B., Toth, G.B., Pavia, H., 2021. Ocean acidification decreases grazing pressure but alters morphological structure in a dominant coastal seaweed. *PLoS One* 16, e0245017.
- Korzen, L., Pulidindi, I.N., Israel, A., Abelson, A., Gedanken, A., 2015. Single step production of bioethanol from the seaweed *Ulva rigida* using sonication. *RSC Adv.* 5, 16223–16229.
- Kruger, N.J., 2009. The Bradford method for protein quantitation. *protein Protoc. Handb.* 17–24.
- Kumar, A., Buia, M.C., Palumbo, A., Mohany, M., Wadaan, M.A.M., Hozzein, W.N., Beemster, G.T.S., AbdElgawad, H., 2020. Ocean acidification affects biological activities of seaweeds: A case study of *Sargassum vulgare* from Ischia volcanic CO<sub>2</sub> vents. *Environ. Pollut.* 259. <https://doi.org/10.1016/j.envpol.2019.113765>.
- Kumar, A., Castellano, I., Patti, F.P., Delle Donne, M., Abdelgawad, H., Beemster, G.T.S., Asard, H., Palumbo, A., Buia, M.C., 2017. Molecular response of *Sargassum vulgare* to acidification at volcanic CO<sub>2</sub> vents: insights from de novo transcriptomic analysis. *Mol. Ecol.* 26, 2276–2290. <https://doi.org/10.1111/mec.14034>.
- Laemmli, U.K., 1970. Cleavage of structural proteins during the assembly of the head of bacteriophage T4. *Nature* 227, 680–685.
- Lichtenthaler, H.K., 1987. [34] Chlorophylls and carotenoids: pigments of photosynthetic biomembranes. *Methods Enzymol.* 148, 350–382.
- Mackey, K., Morris, J.J., Morel, F., Kranz, S., 2015. Response of Photosynthesis to Ocean Acidification. *Oceanography* 25, 74–91. <https://doi.org/10.5670/oceanog.2015.33>.
- Madkour, Fedekar, El-Shoubaky, Gihan, Ebada, Mohamed A., 2019. Antibacterial activity of some seaweeds from the Red Sea coast of Egypt. *Egyptian Journal of Aquatic Biology and Fisheries* 23 (2), 265–274. <https://doi.org/10.21608/ejafb.2019.31016>.
- Masuko, T., Minami, A., Iwasaki, N., Majima, T., Nishimura, S.-I., Lee, Y.C., 2005. Carbohydrate analysis by a phenol-sulfuric acid method in microplate format. *Anal. Biochem.* 339, 69–72.
- Niwa, K., Harada, K., 2013. Physiological responses to nitrogen deficiency and resupply in different blade portions of *Pyropia yezoensis* f. *narawaensis* (Bangiales, Rhodophyta). *J. Exp. Mar. Biol. Ecol.* 439, 113–118.
- Olschlager, M., Bartsch, I., Gutow, L., Wiencke, C., 2013. Effects of ocean acidification on growth and physiology of *Ulva lactuca* (Chlorophyta) in a rockpool-scenario. *Phycol. Res.* 61, 180–190. <https://doi.org/10.1111/pre.12006>.
- Osman, M.E.H., Abo-Shady, A.M., Elshobary, M.E., Abd El-Ghafar, M.O., Abomohra, A. E., 2020. Screening of seaweeds for sustainable biofuel recovery through sequential biodiesel and bioethanol production. *Environ. Sci. Pollut. Res.* 27, 32481–32493. <https://doi.org/10.1007/s11356-020-09534-1>.
- Osman, M.E.H., Aboshady, A.M., Elshobary, M.E., 2013. Production and characterization of antimicrobial active substance from some macroalgae collected from Abu-Qir bay (Alexandria) Egypt. *African J. Biotechnol.* 12, 6847–6858. <https://doi.org/10.5897/AJB10.2150>.
- Osman, M.E.H., Abushady, A.M., Elshobary, M.E., 2010. In vitro screening of antimicrobial activity of extracts of some macroalgae collected from Abu-Qir bay Alexandria. *Egypt. African J. Biotechnol.* 9, 7203–7208. <https://doi.org/10.5897/AJB09.1242>.
- Pachauri, R.K., Allen, M.R., Barros, V.R., Broome, J., Cramer, W., Christ, R., Church, J.A., Clarke, L., Dahe, Q., Dasgupta, P., 2014. Climate change 2014: synthesis report. Contribution of Working Groups I, II and III to the fifth assessment report of the Intergovernmental Panel on Climate Change. *Ippc*.
- Pourjamshidian, R., Abolghasemi, H., Esmaili, M., Amrei, H.D., Parsa, M., Rezaei, S., 2019. Carbon dioxide biofixation by *Chlorella* sp. In a bubble column reactor at different flow rates and CO<sub>2</sub> concentrations. *Brazilian J. Chem. Eng.* 36, 639–645. <https://doi.org/10.1590/0104-6632.20190362s20180151>.
- Reidenbach, L.B., Fernandez, P.A., Leal, P.P., Noisette, F., McGraw, C.M., Revill, A.T., Hurd, C.L., Kübler, J.E., 2017. Growth, ammonium metabolism, and photosynthetic properties of *Ulva australis* (Chlorophyta) under decreasing pH and ammonium enrichment. *PLoS One* 12. <https://doi.org/10.1371/journal.pone.0188389>.
- Rogers, A., Fischer, B.U., Bryant, J., Frehner, M., Blum, H., Raines, C.A., Long, S.P., 1998. Acclimation of Photosynthesis to Elevated CO<sub>2</sub> under Low-Nitrogen Nutrition Is Affected by the Capacity for Assimilate Utilization. *Perennial Ryegrass under Free-Air CO<sub>2</sub> Enrichment*. *Plant Physiol.* 118, 683–689.
- Semesi, I.S., Kangwe, J., Björk, M., 2009. Alterations in seawater pH and CO<sub>2</sub> affect calcification and photosynthesis in the tropical coralline alga, *Hydrolithon* sp. (Rhodophyta). *Estuar. Coast. Shelf Sci.* 84, 337–341. <https://doi.org/10.1016/j.ecss.2009.03.038>.
- Smithson, P.A., 2002. IPCC, 2001: climate change 2001: the scientific basis. Contribution of Working Group 1 to the Third Assessment Report of the Intergovernmental Panel on Climate Change, edited by J. T. Houghton, Y. Ding, D. J. Griggs, M. Noguer, P. J. van der Linden, X. Da. *Int. J. Climatol.* 22, 1144–1144. <https://doi.org/10.1002/joc.763>

- Spoerner, M., Wichard, T., Bachhuber, T., Stratmann, J., Oertel, W., 2012. Growth and thallus morphogenesis of *Ulva mutabilis* (Chlorophyta) depends on a combination of two bacterial species excreting regulatory factors. *J. Phycol.* 48, 1433–1447.
- Sudhakar, M.P., Kumar, B.R., Mathimani, T., Arunkumar, K., 2019. A review on bioenergy and bioactive compounds from microalgae and macroalgae-sustainable energy perspective. *J. Clean. Prod.* 228, 1320–1333. <https://doi.org/10.1016/j.jclepro.2019.04.287>.
- Taylor, J.D., Ellis, R., Milazzo, M., Hall-Spencer, J.M., Cunliffe, M., 2014. Intertidal epilithic bacteria diversity changes along a naturally occurring carbon dioxide and pH gradient. *FEMS Microbiol. Ecol.* 89, 670–678. <https://doi.org/10.1111/1574-6941.12368>.
- Webber, A.N., Nie, G.-Y., Long, S.P., 1994. Acclimation of photosynthetic proteins to rising atmospheric CO<sub>2</sub>. *Photosynth. Res.* 39, 413–425. <https://doi.org/10.1007/BF00014595>.
- Wichard, T., Charrier, B.B., Mineur, F.F.F., Bothwell, J.H., Clerck, O. De, Coates, J.C., De Clerck, O., Coates, J.C., Clerck, O. De, Coates, J.C., 2015. The green seaweed *Ulva*: a model system to study morphogenesis. *Front. Plant Sci.* 6, 1–8. <https://doi.org/10.3389/fpls.2015.00072>.
- Xiao, X., Agustí, S., Yu, Y., Huang, Y., Chen, W., Hu, J., Li, C., Li, K., Wei, F., Lu, Y., 2021. Seaweed farms provide refugia from ocean acidification. *Sci. Total Environ.* 776, 145192.
- Xu, K., Chen, H., Wang, W., Xu, Y., Ji, D., Chen, C., Xie, C., 2017a. Responses of photosynthesis and CO<sub>2</sub> concentrating mechanisms of marine crop *Pyropia haitanensis* thalli to large pH variations at different time scales. *Algal Res.* 28, 200–210.
- Xu, Z., Gao, G., Xu, J., Wu, H., 2017b. Physiological response of a golden tide alga (*Sargassum muticum*) to the interaction of ocean acidification and phosphorus enrichment. *Biogeosciences* 14, 671–681.
- Young, C.S., Gobler, C.J., 2016a. Ocean acidification accelerates the growth of two bloom-forming macroalgae. *PLoS One* 11, 1–21. <https://doi.org/10.1371/journal.pone.0155152>.
- Young, C.S., Gobler, C.J., 2016b. Ocean Acidification Accelerates the Growth of Two Bloom-Forming Macroalgae. *PLoS One* 11, <https://doi.org/10.1371/journal.pone.0155152> e0155152.
- Osman, M.E.H., Abu-Shady, A.M., Elshobary, M.E., 2012. The Seasonal Fluctuation of the Antimicrobial Activity of Some Macroalgae Collected from Alexandria Coast, Egypt, in: *Salmonella - Distribution, Adaptation, Control Measures and Molecular Technologies*. InTech, pp. 173–186. <https://doi.org/10.5772/31907>